Comparison of recycled High Pressure Die Casting AlSi10MnMg alloys for automotive structural components produced in laboratory and industrial environment

A. Bongiovanni, A. Castellero

Aluminum has a key role in the automotive industry, thanks to its lightweight, easy recyclability and corresponding achievable low carbon footprint. Its employment will continue to increase, with castings having the heaviest role. High Pressure Die Casting products are usually produced with secondary material but characterized by low mechanical properties, due to the high Fe content and the detrimental β-Al_5FeSi phases. HPDC structural components, used in the vehicle BiW, are instead cast with primary aluminum for achieving high ductility and strength. The decarbonization of the automotive industry is requiring new alloys with higher recycled amounts and high mechanical properties. The laboratory casting validation and the upscaling to structural components is an important step during the development of new alloys. This study presents the comparison and characterization of a 70% end-of-life scrap AlSi10MnMg alloy, suitable for structural components, first cast in laboratory and then in industrial facility. Casting quality, assessed through evaluation of defects and microstructure, along with the mechanical properties are compared. The industrial process leads to fewer casting defects (cold flakes and cold joints) and rare α-$Al_{15}(Fe,Mn)_3Si_2$ sludge particles. The hardness is affected by the different thickness and the small variation in chemical composition, but in all cases is compliant to with EN 1706 minimum values . The bending test, scarcely sensitive to defects compared to standard tensile test, gives similar ductility results with higher values for the industrial component. The microstructure, hardness and corrosion behavior are comparable to primary alloy's ones.

KEYWORDS: RECYCLE, ALUMINUM ALLOY, HIGH PRESSURE DIE CASTING, ALSI10MNMG, AUTOMOTIVE, STRUCTURAL

INTRODUCTION

Casting is the leading manufacturing technology for automotive aluminum components, thanks to the complex shaped components with good mechanical properties obtained at relatively low price. It represents around 65% of the total aluminum used in a car produced in Europe in 2022 [1] and a steady 25% increase is foreseen by 2030. The housings for E-drive, battery pack and other electric vehicle specific features are the components that lead this growth. High Pressure Die Casting (HPDC) is the most used casting process, representing approximately 60% of the automotive aluminum casting [2]. HPDC products are traditionally the engine, the transmission housing, the oil pan and other components without high mechani-

A. Bongiovanni, A. Castellero
Department of Chemistry, NIS, University of Turin, Italy
*andrea.bongiovanni@unito.it, alberto.castellero@unito.it

cal requirements. The alloys used are usually secondary, obtained easily from recycling and with great advantages as low price and low carbon footprint. Secondary alloys production emits almost 95% less than the primary production route. These alloys, though, possess iron contents around 1%wt and this poses limitations to their use due to the formation of the β-Al_5FeSi phase, characterized by brittle needle shape [3], that greatly limits the elongation at fracture down to 1-2%. High performance components, usually employed in the vehicle Body in White (BiW), require high ductility, because of their need for excellent energy absorption during a possible crash. These structural components are manufactured with primary aluminum alloy, with a strictly limited Fe content and low impurity levels. Ductile alloys are designed for suppressing the detrimental β-phase by alloying other elements such as Mn, Cr and Co. Mn is the preferred Fe-modifier, able to form the polyhedral-shaped α-$Al_{15}(Fe,Mn)_3Si_2$ phase [4] and contribute to avoid die soldering too. Most of the industrial structural ductile alloys have a composition close to the AlSi10MnMg alloy defined in the EN 1706 standard [5]. Suppressing the Fe content by only increasing Mn is not a solution for employing secondary alloys in ductile applications, since the alloy would tend to form large intermetallics that hindered the mechanical properties. Recycled aluminum alloys have not been used up to now in HPDC structural components due to the increase of the tramp elements (Fe, Cu, Zn) during the recycling processes. The need of the automotive industry to reduce the carbon footprint of the raw material used in the vehicles, poses more focus on recycled alloys. Much research is ongoing for developing high-recycled content alloys with high mechanical properties with different alloying correcting elements and varying Fe contents. The research is usually done in universities or research centers with characterizations performed on specimens casted in small HPDC machines. This gives reliable data of the material properties, but the real components casted in industrial facilities could have some behavior divergences, due to the different scale of the part dimension and the manufacturing equipment used. The investment cost of an industrial facility prohibits their massive use in the development phase. In this work, a recycled AlSi10MnMg alloy with 70% End-of-Life (EoL) scrap was firstly casted and characterized in laboratory with a small die, and then a real structural component was produced in industrial environment. The alloy was developed using the EN 1706 – 43500 alloy as reference, the standard name for AlSi10MnMg. The aim is to compare and highlight the differences in the casting quality and the mechanical properties. Casting defects, porosity and microstructure were evaluated, and hardness and bending tests were performed for assessing the strength and ductility of the material. Corrosion validation was performed following automotive standards.

MATERIALS AND METHODS

In this work, one of the six AlSi10MnMg HPDC alloys variants developed and characterized at specimen scale was selected for the manufacturing of a structural automotive component at industrial scale. This alloy contains on average 70% of end-of-life scrap and this value optimizes the balance between the sustainability, due to the high-recycled rate, and the low critical raw material added to the remelted aluminum. When recycling a high amount of EoL scrap, the final composition needs to be adjusted to achieve the correct composition. The main elements to be added are usually Si and Mg, with the latter depending on the alloy design: lowering the Mg content leads to higher ductility, and this was the choice for the alloy developed in the present study. Si content instead needed higher raw material: this alloy had 4.3% Si added to achieve the 9-11.5% Si range required by the standard [5]. Nonetheless, the final Si level was close to the lower limit for the second batch produced for the component casting, as shown in Tab. 1. The variant was designed at the upper tolerances of the detrimental elements of the EN AC 1706 - 43500 alloy, with increased Fe and Cu for assessing the limit of a composition close to the standard, but capable of allowing higher recycling rate. These two elements, with low and strict tolerances, are the most problematic when increasing the recycling rate. A 5250-kN locking force Buhler cold chamber HPDC machine equipped with a VDS vacuum unit (V-HPDC), a shot sleeve with an internal diameter of 60 mm and a stroke of 450 mm was used for producing the specimens for the characterization. The die was designed to fabricate a 180x170 mm flat plate piece with 3 mm thickness (Fig.1a) at 100 mbar residual pressure, obtained by a ProVac CV 300 chill vent. The

melt temperature during casting was 720°C, and the mold was heated by oil circulation to approximately 180°C. The structural components were produced in an industrial environment with a 27000-kN vacuum HPDC machine with 8 channels die thermo-cooling units. The whole casting, measuring 420x550 mm and weighing 9 kg, is shown in Fig1b. The wall thicknesses range from 3 to 8 mm according to the area and vary with the draft angle.

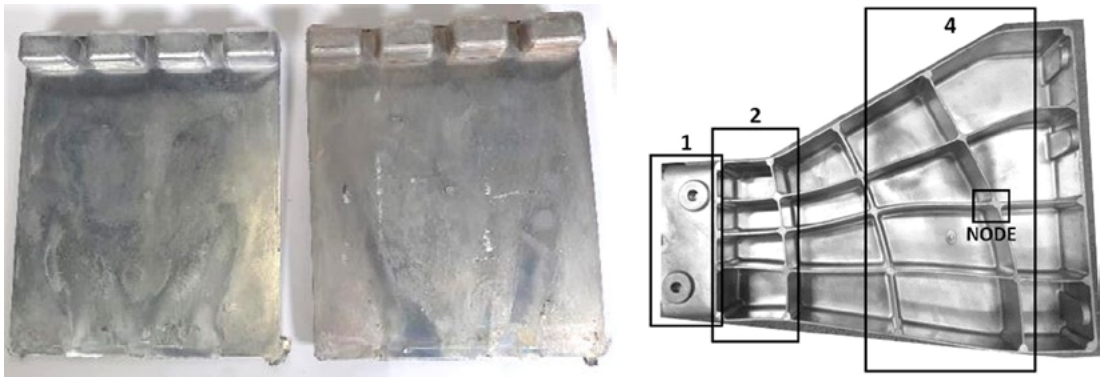

Fig.1 - 180x170x3 mm specimens (A, as cast on the left and after heat treatment on the right) and the structural component (B) analyzed in the four different indicated areas: 1, 2, 4 and node.

The specimens were studied in three temper states: as-cast (F), artificial ageing (T5) and solution and artificial ageing (T6). T5 heat treatment involved two hours at 190°C, while the T6 parameters were solution heat treatment at 490°C for one hour, water quenching and artificial ageing at 230°C for one hour. For the structural component, only T5 was performed for avoiding blistering and distortion, typical of the T6 and that could be problematic for a massive HPDC component. Furthermore, T5 heat treatment leads to yield strength increase that is required by the structural application. This choice is also in line with the trend of the automotive sector of avoiding heat treatment or reducing it, for lower CO_2 emissions and related costs. For this reason, the demonstrator was characterized in the F condition too. The microstructure of the samples was examined using an optical microscope after etching for 10 seconds with a solution of 0.5 ml HF and 99.5 ml distilled H_2O. The cross section of the metallographic samples from the 180x170 specimens was 30x3 mm^2, while the cross sections from the component vary according to the area, ranging from 3 mm to 8 mm thickness. The bending tests were carried out on 50x50 mm samples with test parameters established based on VDA 238-100 standard [6]. A universal tensile machine equipped with a bending device was used for this test. This setup used a 0.2 mm radius. The hardness was measured on the surface of the casted samples for both manufacturing configurations, using an EMTO-TEST DuraVision G5 Brinell machine. The evaluation of the corrosion behavior was performed following the B368 standard using cataphoresis coated plates. ASTM B368 is also known as CASS test (Copper-Accelerated Acetic Acid-Salt Spray (Fog)) and is a typical test used in automotive. For each temper condition, rectangular shape specimens were cut from the component and coated with the anti-corrosion cataphoresis treatment. A linear scratch was then performed on the protective layer for exposing the aluminum substrate to the corrosion test for 168h. The samples for the micrographic, bending and hardness test were cut out from the center of the 180x170 casted plates. The corrosion specimen's location in the die has no influence on the corrosion behavior as they were cut out randomly from the plate. Three specimens per type were used in each test. The samples from the component for the micrographic and hardness test were cut out from different areas of the casting, according to the casting quality obtained by the filling and solidification simulation performed. Four different areas were selected, identified as '1', '2', '4' and 'Node'. The areas are reported in Fig.1b, and 'Node' is the cross section of the casting intersections, identified as the last solidified points in the whole casting. Three specimens per type were used in each test. Bending tests were performed only on area '2' and '4' with 5 mm thickness specimens.

RESULTS AND DISCUSSION

CHEMICAL COMPOSITION

During the casting steps of an aluminum alloy, the chemical composition can slightly change. Compared to other manufacturing methods, casting involves remelting and movements of the liquid metal from one mold to the other, until the final die, where it will solidify in the final shape. From the first solidification as ingot, the aluminum alloy is remelted in the casting facility and the liquid metal is treated for removing the hydrogen entrapped by using a rinsing gas and stirring. Hydrogen is a major factor in the casting porosity due to its very low solubility in solid state aluminum [7]. During this operation, fluxes are used for removing the solid impurities, as oxides and other inclusions, via flotation. The clean molten aluminum is then ready for the casting and is transferred to the holding furnace, from which the material is taken in each casting shot. This is the last step before the final injection, where all the liquid aluminum solidifies in a few seconds, according to the part dimension. During the two solidification steps, the material is in contact with the steel die and with the atmosphere, hence the elements can react with the molds or be oxidized, leading to compositional variations. The chemical composition, measured by Optical Emission Spectroscopy, is shown in Tab.1. The composition was measured in different steps for both the pieces studied: on the ingot and on the casted 180x170 plates; on the ingots, after the degassing and after the casting for the demonstrator component. It can be first noted that the overall composition differs from the specimen to the component. The alloy ingots were produced in two separate times and, even if the same amount of EoL scrap was used, the result is different due to variations in the scrap mix. To achieve the exact same chemical composition, more pure master alloys (i.e. Al-Si, Al-Mn) should have been added, resulting in a decrease of the total recycled percentage and increase of kg CO_2/kg Al. The 1%wt difference of the Si content is the most evident change, but this difference did not lead to castability problems. On the contrary, it could lead to an improved ductility, since eutectic Si particles are brittle and in the absence of defects or more brittle phases, as β-Al_5FeSi phases or sludge particles, are responsible for the cracking propagation [4]. The higher Mg content in the component could lead to higher strength especially after T5 heat treatment, associated with the precipitation hardening effect related to the increase in Mg_2Si phases [8]. Slightly more Fe is present in the second casting, but in both casting types it is observed an increase of the Fe content from the ingot to the final casting. It is known that during recycling the Fe content increases, but in general all melt activities can potentially increase it [3]. Aluminum and iron have a high affinity, inter-diffusing on contact and forming intermetallics that generate die soldering, a major problem in HPDC for the die life [9]. Most aluminum HPDC alloys contain from 0.8% to 1.1% Fe to prevent die soldering, but for high-performance alloys such a high Fe content is impossible: it would form abundant brittle β-AlFeSi intermetallics, which hinders the ductility. Mn is essential for this reason, as it counteracts the die soldering effect and promotes the formation of blocky or Chinese script-like α-$Al_{15}(Fe,Mn)_3Si_2$ compounds instead of β phases [3]. There is a limit to the quantity of Fe and Mn in the alloy because of their tendency to solidify and segregate intermetallics before dendrite formation. The defined Sludge Factor (SF) is an empirical parameter that represents this phenomenon, typically occurring in the holding furnace and/or the shot sleeve [10]. The main intermetallic forming is α-$Al_x(Fe,Mn,Cr)_ySi_z$ and the empirical equation (1) by Gobrecht [11] and Jorstad [12] uses the Fe, Mn and Cr content to calculate it:

$$SF = (1 \times wt\%\ Fe) + (2 \times wt\%\ Mn) + (3 \times wt\%\ Cr) \quad (1)$$

The higher content of Mn in the specimen composition led to a higher SF, resulting in more sludge α-phase particles as will be shown in the micrographic analysis section. Another effect of the foundry processes is the decrease of the Strontium (Sr) content from the ingot to the final casting. Strontium is essential for structural alloys as it promotes the morphological modification of eutectic Si, that is naturally acicular and brittle, improving the elongation at fracture and ductility of the alloy. Even an addition in the order of hundreds part per million of Sr, leads to the spheroidization of the coarse plate-like particles to well-refined fibrous phases [13]. The loss of Sr can be due to oxidation or segregation during the melting phase with subsequent removal during the degassing phase [7, 14].

Tab.1 - Chemical compositions measured by Optical Emission Spectroscopy (OES), Sludge Factor (SF) and recycle content (%).

		Chemical composition [wt. %]										Sludge Factor	Recycle %
		Si	Mg	Fe	Mn	Cu	Zn	Cr	Sr	Sr	Al		
EN 43500		9-11.5	0.15-0.6	<0.2	0.4-0.8	<0.03	<0.07	<0.03	<0.025	<250	bal.	-	-
Alloys design		9-11.5	0.15-0.25	0.2	0.45-0.65	0.03	<0.07	<0.03	<0.025	<250	bal.	-	70
Specimen	ingot	10.54	0.16	0.14	0.59	0.01	0.01	0.01	0.0243	243	bal.	1.35	70
	casting	10.48	0.14	0.17	0.58	0.02	0.01	0.01	0.020	200	bal.	1.36	
Component	ingot	9.45	0.24	0.15	0.46	0.16	0.01	0.01	0.021	210	bal.	1.1	70
	pre-injection	9.33	0.25	0.19	0.49	0.16	0.05	0.01	0.013	130	bal.	1.2	
	casting	9.3	0.26	0.21	0.48	0.15	0.08	0.01	0.0041	41	bal.	1.2	

MICROGRAPHIC EXAMINATION

Defects

HPDC components are characterized by fine-grained structure thanks to the rapid cooling of the liquid aluminum in the die cavity. In this technology, defects are the most detrimental features for the mechanical properties, especially porosities. Their impact is greater than microstructure brittle phases, which have a heavier effect on slower solidification casting methods, like low pressure die casting. Despite the vacuum assisted operation, the high turbulence during the filling shot can produce numerous defects: casting (i.e. cold joints and cold flakes), solidification (shrinkage porosity) and air-entrapment (gas porosity) defects. Casting the same material in two different manufacturing environments can result in different presence and distribution of the defects.

Figure 2a-b shows the porosities in the laboratory casted specimens before the heat treatment and after T5, while Fig.2c-d the porosities in the industrial component in area 2 and in the node. It can be noted that the T5 heat treatment does not enhance the porosities at macroscopic level, as can happen after a T6 heat treatment [15]. Gas entrapment pores are the most frequent in the specimens, characterized by spheroidal shape and in general small and dispersed, with only few big voids as in Fig.2b. Shrinkage macro-porosity is observed in the component in the last solidifying areas and in the thicker sections, as in area 4 and in the nodes (Fig.2d) with sizes up to 1 mm. Gas pores are instead present throughout all the areas of the casting. Laboratory plates macrography in Fig.2a-b have a similar appearance to the industrial component in Fig.2c. What they have in common is the rapid solidification, derived by the low thickness and small melt aluminum volume to be cooled of the plate specimen, and the die of the component which was designed for having faster solidification and resulting better properties in these areas. The material solidifies at last in the thickest areas, as in the nodes, where the cross-section thickness is almost 20 mm. The volume shrinkage of aluminum is not balanced enough and generates macro void, as visible in Fig.2d.

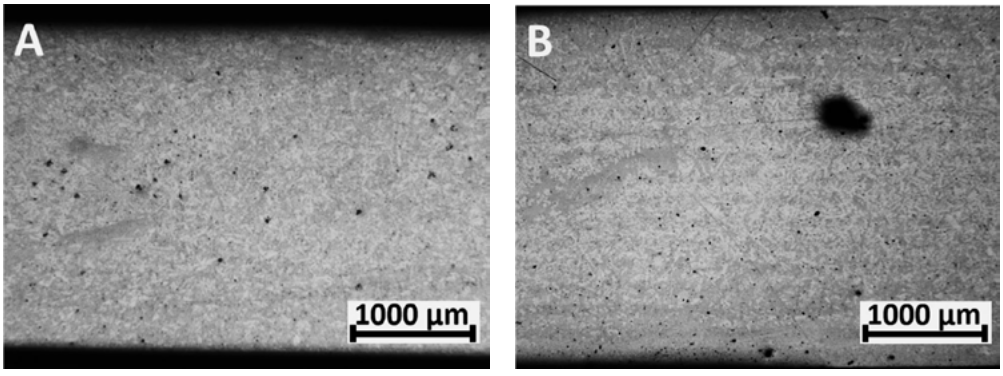

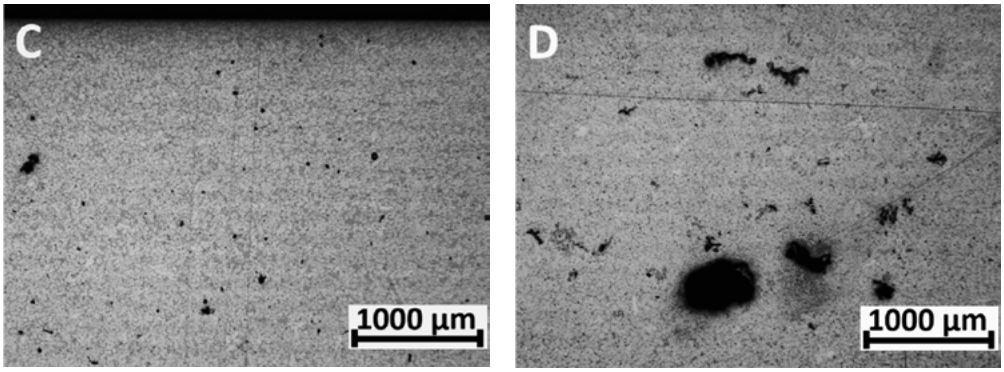

Fig.2 - Optical micrographs showing the porosities in the as-cast (a) and T5 (b) temper, for the laboratory casted specimen, and in the first solidifying areas 1 and 2 (c) and last solidifying area, the nodes (d), for the industrial casting component.

The differences in casting quality peak when observing the other casting defects. Figure 3a shows how, even at low magnification, cold flakes and cold joints are visible in the specimen's cross section. Cold flakes are formed during the injection of the liquid metal in the die cavity, prior to solidification in the die cavity. As the shot sleeve is filled, a layer of aluminum initially solidifies and oxidizes in the cold chamber. When the plunger injects the molten material into the die, this solidified layer breaks into numerous small particles around the casting [16]. The casting component (Fig.3b) is more homogeneous with only some primary aluminum dendrites, that are solidified externally to the die and are characterized by a bigger dimension. While the defects from the laboratory casting are continuous and found in all the sample sections analyzed, only few cold flakes and cold shots were observed in the industrial casting. Fig.3c and Fig.3d reports two examples of casting defects, cold flakes, that show similar appearance. The dendritic structure is coarser than the surrounding bulk and both contains sludge intermetallic particles, as better shown in the insets of the figures.

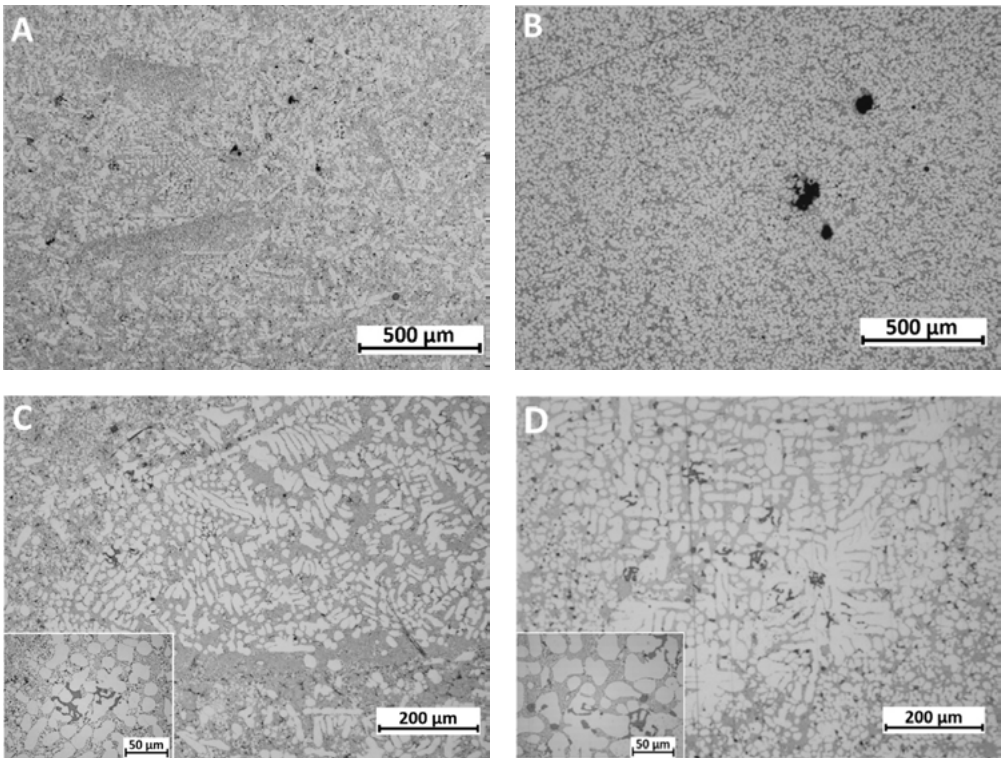

Fig.3 - Microstructure of the cross sections in the specimen (a) and in the component (b), showing the average casting quality observed. Examples of cold flake observed in the specimen (c) and in the component (d).

Other defects often seen in the specimens are cold joints, visible even at low magnification as the darker flat areas in Fig.3a. These occur when, during the die filling, a molten metal flow with a superficial oxide layer encounters another liquid front. The produced interface is a discontinuity in the material that can facilitate the initiation or the propagation of a crack. During T6 heat treatment, the discontinuity is highlighted and the matching fronts can separate, generating a linear void [15].

Microstructure

The deviations in the chemical composition and the casting quality leads to differences in the microstructure and in the phases present. Figure 4 clearly shows the presence of fine and coarse α-$Al_{15}(Fe,Mn)_3Si_2$ intermetallic compounds in the specimen (a) and in the component (b). The Chinese script-like coarse white particles are called sludge particles and solidify in the shot sleeve or during the transfer from the cold chamber to the shot sleeve [13]. These are abundant in the specimen's microstructure, characterized by a higher SF and more casting defects. The industrial component shows fine intermetallics, formed only during the solidification in the die. Their shape is mostly blocky and equiaxial, with a dimension in the order of the μm, while the sludge particles have a Feret diameter around 40 μm. Only few coarse α-AlSiMnFe phases were observed in the component, apart from the ones observed in cold flakes as in Fig.3d. These volumes of material solidify outside the die and with lower cooling rates, a combination that helps the formation of the sludge particles. The Mn content in both parts is enough to suppress the undesired β-Al5FeSi phase, characterized by acicular shape and very brittle. Only few of these intermetallics were observed in the thickest areas of the component, but the big porosities shown in Fig.2d represents the main problem. No β-AlFeSi phases were observed in the specimens given the lower constant thickness and the higher Mn content. This is proven by the fact that all the Fe detected in the microstructure is bonded with Mn, as demonstrated by the SEM/EDS analysis maps in Fig. 5.

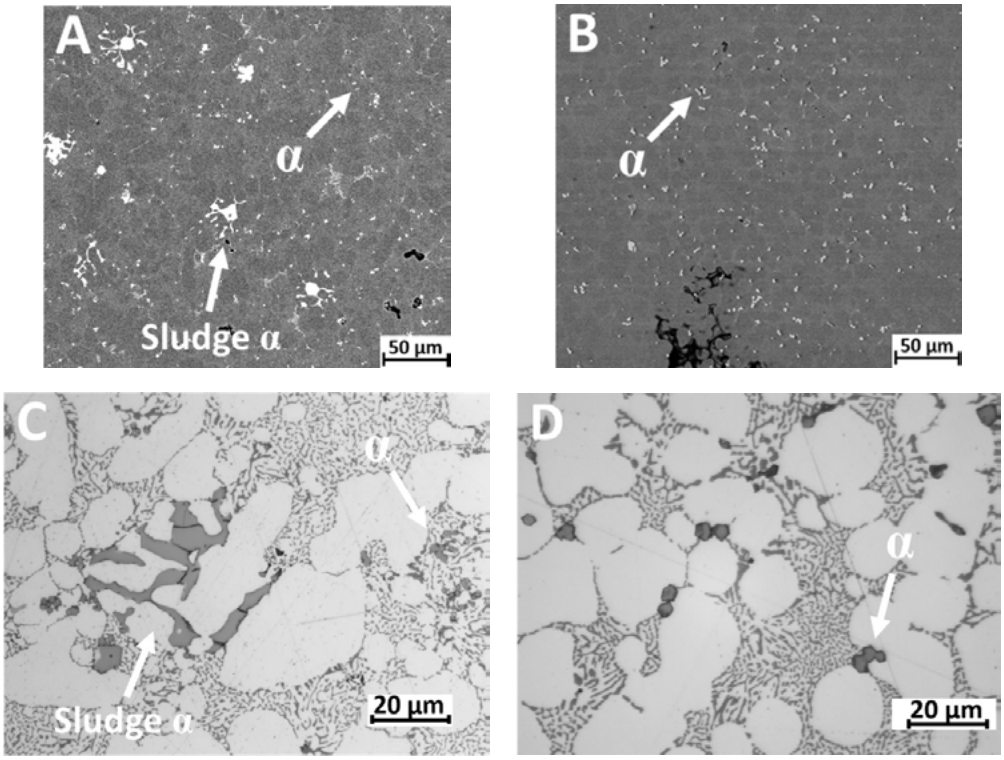

Fig.4 - Sludge and fine α-$Al_{15}(Fe,Mn)_3Si_2$ intermetallic phases in the specimen (a, c) and the component (b, d) microstructure.

The eutectic silicon particles did not show any relevant modification after the T5 in both castings, unlike the T6 treatment that effectively spheroidized the fibrous morphology, as demonstrated in a previous characterization of the specimens [15]. The effect of the T5 heat treatment can be noted in the Mg_2Si particles evolution. Figure 5 shows the EDS maps after T5 for the specimen (a) and the component (b), and it can be noted how the components have more Mg concentrated traces, sign of more Mg_2Si particles. The minor Mg content shown in Tab.1 of the specimens leads to this difference. No relevant change was observed in the specimens Mg_2Si particles after the T5, given the low amount of Mg. An increase in dispersion and dimension of Mg phases was instead visible after the heat treatment for the component.

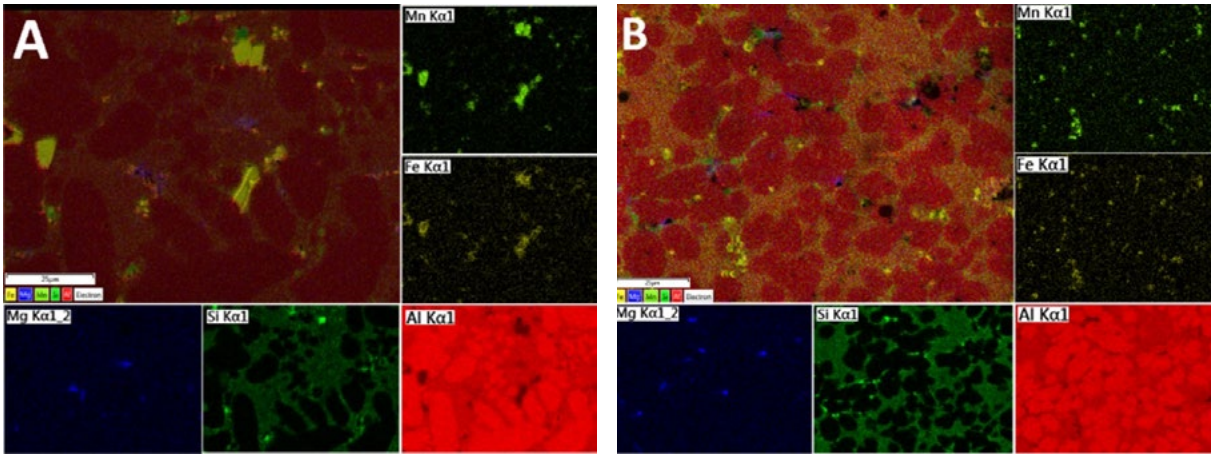

Fig.5 - EDS maps of the microstructure after T5 heat treatment of the specimens (a) and the component (b).

MECHANICAL PROPERTIES

Hardness

Table 2 reports the hardness measured on the surface of both the specimen plates and the structural component, for all the heat treatment conditions. The values reported for the component are the average of all the measurements performed throughout the component areas shown in Fig.1b, since no difference was noted in the surface hardness. Observing the specimen values between the three tempers, it can be appreciated the T6 effect that improves the ductility, thus decreasing the strength and the relative hardness of the material. T5 did not lead to a relevant improvement, with only a 2 HB increase, while the 10-15 HB delta of the component met the expectations. This could be related to the chemical composition of the specimens, which had a Mg content of 0.14%wt., too low for forming enough new Mg_2Si precipitates after T5. The hardness enhancement is clear in the component, with 11 HB more than in the as-cast, thanks to the higher Mg content of 0.26%wt. As also shown in Fig.5 by the EDS analysis, very few Mg2Si phases were noted in the specimens while they are more present in the component, with a dimension and dispersion growth after T5. A relevant difference lies in the as-cast values between the two castings. An explanation of this difference could be the thickness of the two analyzed parts, with the 180x170mm plates being 3 mm thick and the components ranging from 3 to 8 mm. The minor thickness leads to lower solidification and cooling time, resulting in higher mechanical properties. A similar behavior is noted in the skin of the aluminum castings, as reported in a study of Yang [17], which proves how the superficial material in HPDC part has higher hardness than the core. The higher cooling rates of the material in direct contact with the die leads to a finer microstructure and, thus the decreasing thickness enhances the skin-effect on the mechanical properties. A second contributor to this increase in the as-cast state is the higher content of α-$Al_{15}(Fe,Mn)_3Si_2$ intermetallics, both in fine and coarse dimension. All the hardness values reported in Tab.2 satisfy the minimum hardness values specified by the EN 1706 standard for the 43500 – AlSi10MnMg alloy, i.e., 65 HB for F temper, 80 HB for T5 and 60 HB for T7 that can be considered a reliable minimum limit for T6 too [5].

Tab.2 - Mechanical properties: Brinell hardness results performed on the surface of the casting and in the cross-section.

	Heat Treatment	Hardness Brinell	
		Average	St.Dev
Specimens	As-Cast	85.3	1.6
	T5	87.2	2.6
	T6	67.5	1.0
Component	As-Cast	77.6	1.5
	T5	88.9	1.4

Bending

The results of the bending test are reported in Table 3 and well correlates with the hardness results. Three point bending test assesses the local ductility of the material, compared to the global ductility measured with tensile test along the entire gauge length of the specimen. This helps to reduce the influence of the casting defects on the elongation at fracture, since only part of the resistant section is under tension and enhances the skin-effect role in improving the mechanical properties. Comparing the results from the specimens and the component, a small improvement in bending angle is noted in the industrial casted material. The better casting quality, observed by the lower casting defects in Fig.3, leads to higher ductility, and in the first solidifying area, i.e. Area 2, this effect is more evident. This deviation can be also caused by the higher content of α-$Al_{15}(Fe,Mn)_3Si_2$ sludge intermetallic observed in Fig.4 of the specimens. The high Mn content combined with the relatively high 0.17%wt. Fe leads to high SF and the formation of many sludge particles. As demonstrated by Bosch et al. [4], when the Mn content is too high and leads to α-AlSiMnFe sludge formation, the multiple cracking of the sludge particles becomes the crack initiation mechanism, reducing the ductility. A similar behavior was observed in the hardness, with an increase in the specimen's values in the as-cast state. Comparing the standard deviation of the values in as-cast and T5 conditions from the two castings, it can be better appreciated the defect effect on the results. The scattering of the values is constant on the component with a low St.Dev., while the specimens show higher dispersion. However, the averages obtained in the two tempers are comparable and show the same trend after T5. The T6 heat treatment was performed only in the laboratory castings, and the effect of the eutectic Si spheroidization is clear in the improvement of local ductility. Regardless of the typical blistering problem of HPDC parts after T6 [8] and the porosity increase, the St.Dev. decreases drastically. The increment of ductility is enough to have a homogenization effect on the material, with very low standard deviation.

Tab.3 - Mechanical properties: bending angle with standard deviation.

	Heat Treatment	Area	Bending VDA 238-100	
			Average	St.Dev
Specimens	As-Cast	-	22.3	7.0
	T5	-	12.9	8.6
	T6	-	58.5	0.6
Component	As-Cast	2	23.7	2.5
		4	21.8	2.2
	T5	2	15.7	2.1
		4	13.5	1.7

CORROSION BEHAVIOR

In the automotive industry, structural components of the Body-in-White (BiW), like the one examined in this study, are always treated with anti-corrosion coatings. The cataphoresis process, also known as e-coating, involves electrochemically applying an epoxy-type coating to a metal component. This method is the primary means of protection of BiW parts from corrosion, but it is essential to ensure the compatibility and strong adhesion of the cataphoresis coating to the material. A major concern for high-recycled content aluminum alloys is the copper (Cu) level, which could lead to corrosion and compatibility issues with the cataphoresis coating. During the ASTM B368 test, a standard tape is applied to the preformed scratch and then pulled off to measure the width of the removed material. Specifically, the groove left after removing the tape must be less than 1.5 mm wide. All specimens passed the test, showing similar corrosion behavior with no differences before and after heat treatment and regardless of the manufacturing environment. The studied alloy had a Cu content of 0.02% in the first batch of ingots for the specimens, while 0.15% in the second one for the industrial component. The latter value exceeds the strict limit set by the EN 1706 standard (max 0.03%), but no incompatibility or corrosion issues were observed in the test.

CONCLUSIONS

In the present study a recycled AlSi10MnMg aluminum alloy was casted and characterized in two different environments: in a laboratory with a 5250-kN HPDC machine and in an industrial facility with a 27000-kN machine. The alloy was designed for achieving the high mechanical properties required by a structural automotive component. The comparison was performed for assessing the differences in casting quality and properties obtained when developing a new recycled alloy in casted specimens in laboratory and then in a structural component in an industrial facility. The overall casting quality from the two environments shows relevant differences. Even if the laboratory casted part is small and its shape does not include corners and ribs as in the industrial component, the number of casting defects is higher. The natural high productivity and optimized process of an industrial environment made the difference in the final casting quality. The duration and efficiency of the casting process phases - remelting, material movement and especially the longer duration of the liquid aluminum transfer from the holding furnace to the shot sleeve - made at laboratory level led to most of the defects.

- The chemical composition obtained by recycling a fixed amount of EoL scrap (i.e. 70%) can lead to compositional differences between different batches. The composition of the scrap mix used is not a constant variable.
- Gas-entrapment porosity is a "natural" defect of HPDC, and no difference lies between the two foundry environments. Casting quality defects, such as cold flakes and cold joints, were frequent in the laboratory casting , while almost absent in the industrial component.
- The higher SF and lower casting quality of the laboratory specimens, led to high sludge α-$Al_{15}(Fe,Mn)_3Si_2$ intermetallics presence. Only fine compact α-AlFeMnSi phases were observed in the structural component.
- No β-Al_5FeSi were observed thanks to the well-balanced Fe/Mn content and the low thickness of both castings. Only few were observed in the core of the component's nodes.
- Low amounts of Mg_2Si phases were found in the specimens even after T5, due to the low amount of Mg (0.14%wt.). Higher distribution and dispersion of strengthening Mg phases were observed in the component, having a Mg content of 0.26%wt.
- The hardness in the as-cast temper is higher for the specimens due to the lower thickness, while after T5 the component hardness is higher due to the major contribution of the Mg_2Si phases. The average values obtained in all the heat treatment conditions (as-cast, T5, T6) and for both casting types satisfy the minimum values indicated in the EN 1706 standard.
- Bending test was used for assessing the ductility of the material and resulted in being little sensitive to casting defects, thanks to the skin-effect and the local assessment of the test. The same behavior to T5 and similar values even in the as-cast state were obtained. The standard deviation in the specimen castings is much higher due to the casting defects and sludge particles. The T6 treatment enhanced the ductility enough to overcome the defect effect.
- Corrosion resistance is provided by cataphoresis coating

for automotive structural components and the adhesion compliance must be guaranteed. Even with Cu level exceeding the EN 1706 upper limit, the material studied is compliant to the automotive standards.

ACKNOWLEDGEMENT

The results presented in this work have been partially obtained within the framework of project Horizon 2020 SALEMA, Grant Agreement no. 101003785.
The author would like to thank CRF Centro Ricerche Fiat – Stellantis, partner of the SALEMA project, for the laboratory support and the permission to publish the results.
The author acknowledges the support from the Project CH4.0 under the MUR program "Dipartimenti di Eccellenza 2023-2027" (CUP: D13C22003520001).

BIBLIOGRAFIA

[1] Aluminum content in European Passenger Cars, Public Summary, 2023, Ducker Frontier.
[2] Bonollo, F., Gramegna, N. & Timelli, G. High-Pressure Die-Casting: Contradictions and Challenges. JOM 67, 901–908 (2015).
[3] Taylor, John. (2012). Iron-Containing Intermetallic Phases in Al-Si Based Casting Alloys. Procedia Materials Science. 1. 19–33
[4] Bösch, Dominik & Pogatscher, Stefan & Hummel, Marc & Fragner, Werner & Uggowitzer, Peter & Göken, Mathias & Höppel, H.W. (2014). Secondary Al-Si-Mg High-pressure Die Casting Alloys with Enhanced Ductility. Metall and Mat Trans A. 46.
[5] ISO 1706:2020, "Aluminum and aluminum alloys – Castings – Chemical composition and mechanical properties", Int. Organ. Stand, 2020.
[6] VDA 238-100 test specification draft: Plate bending test for metallic materials. 12/2010
[7] Podaril, M.; Prášil, T.; Majernik, J.; Kampf, R.; Socha, L.; Gryc, K.; Gráf, M. Aluminum Melt Degassing Process Evaluation Depending on the Design and the Degree of the FDU Unit Graphite Rotor Wear. Materials 2022, 15, 4924
[8] J.Y. Zhang, E. Cinkilic, X.J. Huang, G.G. Wang, Y.C. Liu, J.P. Weiler, A.A. Luo, Optimization of T5 heat treatment in high pressure die casting of Al–Si–Mg–Mn alloys by using an improved Kampmann-Wagner numerical (KWN) model, Mater. Sci. Eng. A, 865 (2023) 144604
[9] Kohlhepp, M.; Uggowitzer, P.J.; Hummel, M.; Höppel, H.W. Formation of Die Soldering and the Influence of Alloying Elements on the Intermetallic Interface. Materials 2021, 14, 1580.
[10] Ceschini, Lorella & Morri, Alessandro & Toschi, Stefania & Bjurenstedt, Anton & Seifeddine, Salem. (2018). Influence of Sludge Particles on the Fatigue Behavior of Al-Si-Cu Secondary Aluminium Casting Alloys. Metals. 8. 268
[11] Gobrecht, J. Settling-out of Fe, Mn and Cr in Al-Si casting alloys. Giesserei 1975, 62, 263–266. 15.
[12] Jorstad, J. Understanding sludge. Die Cast. Eng. 1986, 30, 30–36
[13] Dahle A.K., K. Nogita, S.D. McDonald, C. Dinnis, L. Lu, Eutectic modification and microstructure development in Al–Si Alloys, Mater. Sci. Eng.: A 413–414 (2005) 243–248.
[14] Ganesh, M R & Reghunath, Nikhil & J.Levin, M. & Prasad, Adarsh & Doondi, Sanapala & Shankar, Karthik. (2021). Strontium in Al–Si–Mg Alloy: A Review. Metals and Materials International.
[15] Bongiovanni, A.; Da Silva, M.; Castellero, A. Comparison of As Cast and T6 heat treatment on high end-of-life-scrap secondary aluminium alloy for High-Pressure Die Casting automotive structural components. La Metallurgia Italiana, 2024, 115(4):50-56.
[16] Ahamed, Aziz & Kato, Hiroshi. (2008). Effect of cold flakes on mechanical properties of aluminium alloy die casts. International Journal of Cast Metals Research - INT J CAST METALS RES. 21. 162-167.
[17] Yang, K.V., Nagasekhar, A.V., Lumley, R., Caceres, C.H.: The skin effect of high pressure die casting Al alloys. Proceedings of the 12th International Conference on Aluminum Alloys, pp. 687–692 (2010).

TORNA ALL'INDICE >